

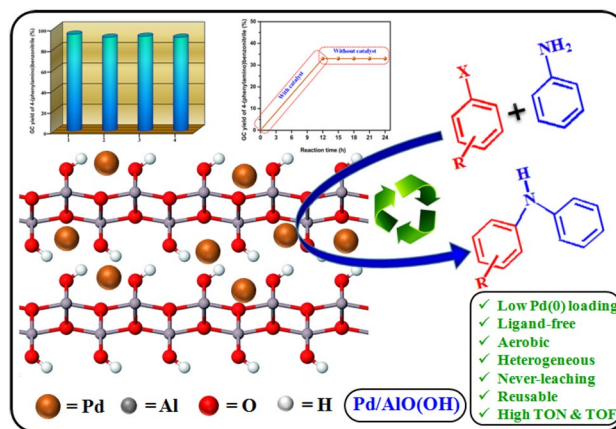
Pd/AIO(OH): A Heterogeneous, Stable and Recyclable Catalyst for N-Arylation of Aniline Under Ligand-Free Aerobic Condition

Sundaram Ganesh Babu^{1,2}  · Balakumar Emayavaramban¹ · Peter Jerome¹ · Ramasamy Karvembu¹

Received: 14 March 2017 / Accepted: 2 August 2017
© Springer Science+Business Media, LLC 2017

Abstract Many synthetic methods have been reported to construct an aryl-nitrogen bond. But they mainly suffer from the usage of expensive ligands. Herein, we report highly effective, heterogeneous, reusable and ligand-free nanocatalyst for the Buchwald-Hartwig coupling reaction under aerobic condition. Wafer-like structure with nano-porous nature of AIO(OH) was identified with TEM and BET surface area analyses. Zero valent Pd nanoparticles (with less than 10 nm crystallite size which strongly evident from TEM analysis) were observed in XRD pattern, which was further confirmed by XPS studies. The reaction conditions were optimized and the scope of the reaction was extended with various aryl halides and aniline using low amount of Pd (0.31 mol%) based heterogeneous catalyst. Heterogeneity, reusability and stability (confirmed by XRD) were found to be reasonable. Use of meagre amount of Pd and the ligand-free aerobic condition make this system economically as well as environmentally feasible.

Graphical Abstract



Keywords Pd/AIO(OH) · Buchwald–Hartwig coupling · Ligand-free · Reusable · Heterogeneous · Aerobic condition

1 Introduction

Amines are ubiquitous in biology. Many neurotransmitters are amines, including epinephrine, norepinephrine, dopamine, serotonin and histamine. Many amine-based drugs are designed to mimic or to interfere with the action of natural amine neurotransmitters. Ephedrine and phenylephrine, as amine hydrochlorides, are used as decongestants. Due to their interesting physiological activities, secondary amines are extremely important pharmacophores in numerous biologically active compounds, which have greatly been touted in drug discovery where the secondary amine can be utilized as important scaffolding for further manipulations [1]. Secondary amines are also a vital class of intermediates in the preparation of natural products. With the growing repertoire

✉ Sundaram Ganesh Babu
Sundaram.Babu@uct.ac.za

✉ Ramasamy Karvembu
kar@nitt.edu

¹ Department of Chemistry, National Institute of Technology, Tiruchirappalli 620015, India

² Catalysis Institute, Department of Chemical Engineering, University of Cape Town, Cape Town 7701, South Africa

of biologically relevant nitrogenous molecules, there is the need for efficient synthetic methods to produce secondary amines as it is the more useful intermediates [2–4].

Several methods have been published for the synthesis of secondary amines. Palladium-based homogeneous catalytic systems developed using a palladium salt with organic ligands were found to possess superior catalytic performance for the N-arylation of amines. For instance, aryl triflates undergo N-arylation of amine (with aliphatic as well as aromatic amines) in the presence of palladium-allyl complex [5]. A general and efficient method for the N-arylation of amine catalyzed by palladium-dinaphthol complex was reported by Dai et al. [6]. Similarly, a variety of aryl amines was synthesized from the reaction of aryl halides with amines in the presence of a catalytic amount of palladium acetate [7]. All these systems are homogeneous which possesses some disadvantages such as use of expensive and less-stable ligands, and toxic solvents, besides the lack of reusability.

Heterogenization of homogeneous inorganic complexes is one of the smart techniques to overcome the drawbacks of homogeneous catalytic systems [8–10]. In this regard, an efficient Buchwald–Hartwig reaction catalyzed by SPI-ONs-Bis(NHC)-Pd(II) catalyst was reported by Ghotbinejad et al. in which N-heterocyclic dicarbene palladium(II) complex was anchored on superparamagnetic iron oxide nanoparticles [11]. However, developing a ligand-free Pd-catalyzed Buchwald–Hartwig coupling remains a great challenge. Recently, Arisawa and co-workers developed a ligand-free Buchwald–Hartwig aromatic amination of aryl halides catalyzed by low-leaching and highly recyclable sulfur-modified gold-supported palladium (SAPd) material in xylene at 130 °C [12]. To the best of their knowledge SAPd-catalyzed aromatic amination is the first ever ligand-free Buchwald–Hartwig C–N coupling system. Hence, we aspire to develop heterogeneous nanocatalytic system for the preparation of the secondary amines under ligand-free condition. Nanocatalytic system combines the advantages of both the homogenous and the heterogeneous catalysis. Nanocatalysts have high surface to volume ratio which increases the contact between the active site and reactant molecules resulting in increase in the yield of the product. Moreover, nanocatalysts are insoluble in common solvents and hence the catalyst can be recovered easily by simple filtration/centrifugation.

Boehmite, AlO(OH) is one of the potential supporting materials for metal nanoparticles (MNPs). For example, aerobic oxidation of a wide range of alcohols to corresponding carbonyl compounds was successfully achieved using Au/AlO(OH) nanocatalysts [13]. Similarly, Rh/AlO(OH) can be used as a catalyst for the hydrogenation of arenes and ketones to produce the corresponding alkanes and alcohols, respectively. Importantly, the catalyst can be reused for ten

times without any activity loss [14]. Recently, copper on boehmite was reported as an effective catalyst for the oxidation of alcohols in water at room temperature [15] and also for the formation of β -enamino ketones/esters under solvent, ligand and base free conditions [16]. Pd/AlO(OH) was found to be an efficient nanocatalyst for some of the industrially important organic transformations such as the conversion of alkene to alkane [17], aryl halide to benzene [18], oxime to amine [19], silane to silyl alcohol [20], and nitro benzene to aniline [21], and one spot synthesis of imines [22] and selective alkylation of ketones with alcohols [23]. Herein, we report an effective procedure for the N-arylation of aniline using aryl halides in presence of recyclable heterogeneous Pd/AlO(OH) catalyst under ligand-free aerobic condition.

2 Experimental

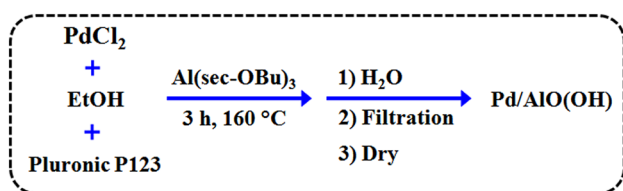
2.1 Materials and Methods

All the reagents used were of chemically pure and/or analar grade and all the glassware were dried overnight in an oven before use. Commercial grade solvents were distilled as per standard procedures and dried over molecular sieves before use. All other chemicals were purchased from Aldrich and were used without further purification.

Powder X-ray diffraction (XRD) measurements were performed on a Rigaku Ultima-III X-ray diffractometer using Cu K α radiation. Scanning electron microscopy-Energy dispersive spectroscopy (SEM-EDS) and transmission electron microscopy (TEM) analyses were done in Hitachi instruments. The BET surface area and pore diameter distributions were analyzed on Gemini V surface area and pore size analyzer. X-ray photoelectron spectra (XPS) (Kratos Axis-Ultra DLD, Kratos Analytical Ltd, Japan) were recorded to confirm the chemical state of Pd in Pd/AlO(OH). During the XPS analysis, the sample was irradiated with Mg K α ray source. ICP analysis was performed using Perkin Elmer Optima 5300 DV ICP-OES instrument.

2.2 Pd/AlO(OH) Catalyst Preparation

PdCl₂ (200 mg, 2.3 mmol), pluronic P123 (4.0 g) and absolute ethanol (10 mL) were added in 100 mL round bottom flask equipped with a condenser. The mixture was stirred for 30 min at 27 °C. Then, Al(O-*sec*-Bu)₃ (9.1 g, 37 mmol) was added carefully. After being stirred at 160 °C for 3 h, 3 mL of water was added. The reaction mixture was stirred further for 30 min at 160 °C, cooled down and kept at room temperature for 3 h. The resulting solid was filtered, washed



Scheme 1 Schematic representation for the preparation of Pd/AIO(OH)

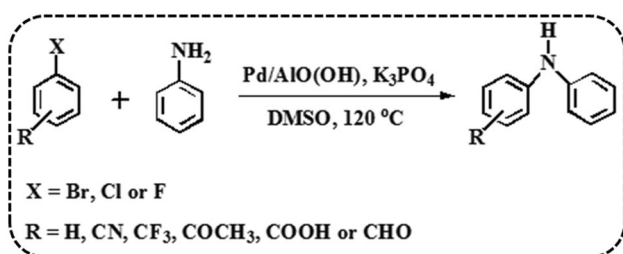
with acetone, and dried at 120 °C for 2 h to give an ash colour powder (3 g, 3.2 wt% of Pd) (Scheme 1) [23].

2.3 N-arylation of Aniline

A mixture of aryl halide (1 mmol), aniline (1.2 mmol), Pd/AIO(OH) (0.31 mol%), potassium phosphate (1.5 mmol) and DMSO (3 mL) was stirred at 120 °C for the appropriate time (Scheme 2). After completion of the reaction as indicated by TLC or GC, the reaction mixture was centrifuged to recover the catalyst. The centrifugate was diluted with 3 mL of ethyl acetate and treated with 3 mL of HCl (2 M) to separate the product. Then, the organic layers were dried over anhydrous sodium sulphate, filtered, concentrated, and the resulting product was purified by column chromatography using hexane:ethyl acetate (80:20) mixture.

2.4 GC Conditions

GC (Shimadzu-2010) was equipped with 5% diphenyl and 95% dimethyl siloxane Restek-5 capillary column (60 m length, 0.32 mm dia) and a flame ionization detector (FID). The initial column temperature was increased from 100 to 230 °C at the rate of 20 °C/min and hold for 11 min. Nitrogen gas was used as a carrier gas. The temperatures of both injection port and FID were kept constant at 250 °C during the product analysis.



Scheme 2 Schematic illustration for the Pd/AIO(OH)-catalyzed N-arylation of aniline

3 Results and Discussion

3.1 Characterizations

Powder XRD pattern of Pd/AIO(OH) catalyst is illustrated in Fig. 1. The relatively broad peaks at Bragg's angle of 14.78°, 28.06°, 49.82°, 56.36°, 64.92°, 68.20° and 72.14° correspond to the (020), (120), (200), (151), (231), (260) and (251) planes of the orthorhombic γ -AIO(OH) solid matrix, respectively (JCPDS card # 21-1307) [24, 25]. The additional two peaks centred at 40.08° and 46.58° represent the Bragg reflections from the (111) and (200) planes of zero valent and cubic structured palladium nanoparticles (Pd NPs) (JCPDS card # 88-2335); showing clear immobilization of Pd(0) NPs onto the surface of γ -AIO(OH) support [26, 27].

Figure 2a represents the SEM image of Pd/AIO(OH), which clearly shows tiny Pd NPs. The present SEM image is similar to the previously reported SEM images of Pd/AIO(OH) [28, 29]. Additionally, the elemental composition of Pd/AIO(OH) catalyst was identified by EDS analysis (Fig. 2b). The EDS spectra showed all the expected elements Pd, Al, C and O. The weight percentage of Pd was found to be 3.32 (inset of Fig. 2b). Furthermore, the weight percent of Pd content in the catalyst was also analyzed with ICP and the value was found to be 3.46 which is in good agreement with the EDS analysis. TEM images of pristine AIO(OH) (Fig. 3a) and Pd/AIO(OH) (Fig. 3b, c) are illustrated. It is evident from Fig. 3a that pure AIO(OH) has a wafer structure. It is worth to mention here that AIO(OH) is highly transparent as can be seen from Fig. 3b also. Aggregated Pd NPs were identified in some places over AIO(OH) support (Fig. 3b). Nevertheless, the separated individual Pd NPs were found in

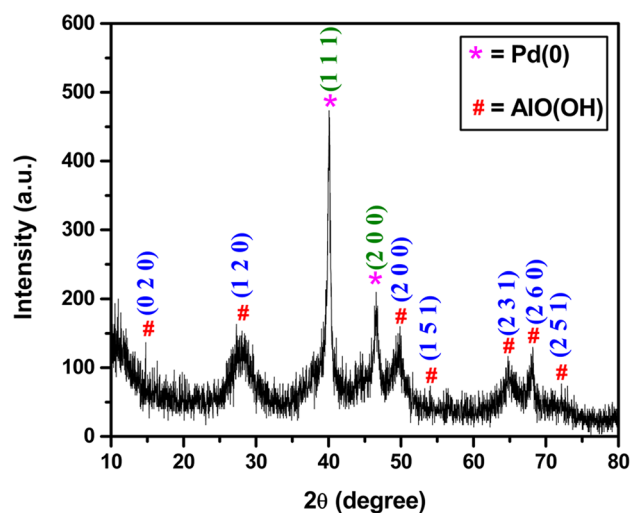


Fig. 1 Powder XRD pattern of Pd/AIO(OH)

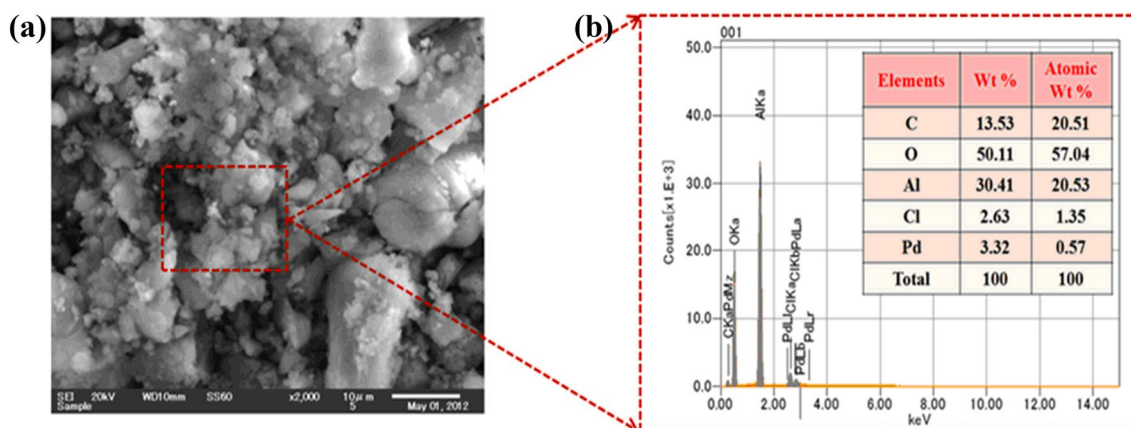


Fig. 2 a SEM and b EDS spectrum (*inset* elemental weight percentage) of Pd/AIO(OH)

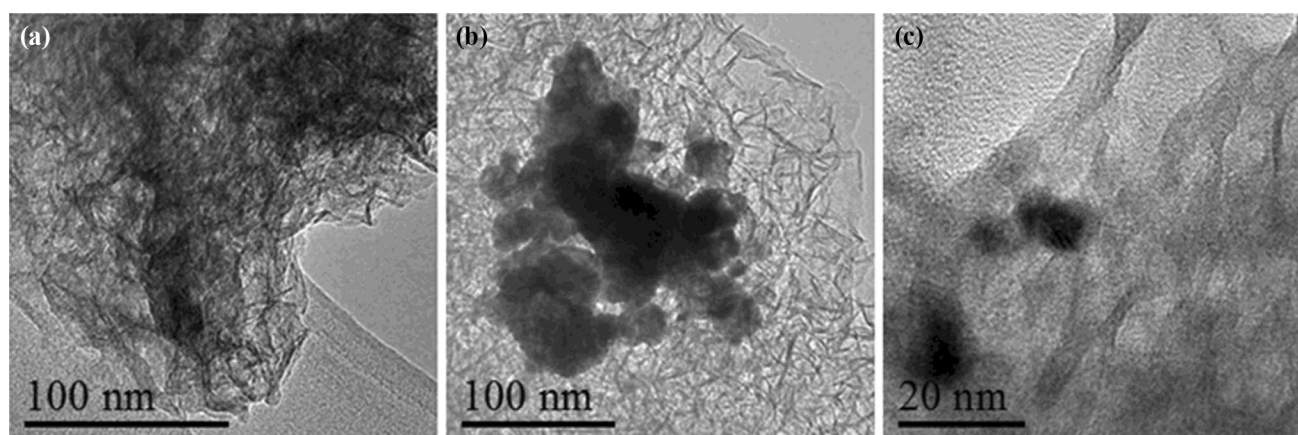


Fig. 3 TEM images of a pristine AIO(OH) and b and c Pd/AIO(OH)

many places (Fig. 3c). The higher magnification image illustrated in Fig. 3c revealed the smaller crystallite size of Pd NPs (10 nm), which is important for achieving good catalytic activity.

Because of the wafer structure and porous nature of AIO(OH), the surface area was expected to be high [30]. As expected, the BET surface area of Pd/AIO(OH) was estimated to be 317.09 m²/g from the BET adsorption–desorption graph, given in Fig. 4a. Furthermore, Pd/AIO(OH) catalyst possesses narrow pore size distribution and the mean pore diameter was found to be 3.5 nm (Fig. 4b). This clearly supports the presence of nano-porosity in Pd/AIO(OH). Conversely, the already reported crystalline boehmite nanotubes exhibited a broad peak in the pore size distribution graph corresponding to the pore diameter value of 10–50 nm with a maximum at 24.3 nm [31]. Hence, the preparation procedure adopted for the synthesis of the present catalyst made a noteworthy influence in attaining the nano-porous wafer AIO(OH) support. All the significant properties such as high

surface area, nano-porous structure and less than 10 nm size Pd NPs played a vital role in excellent catalytic performance (with meagre amount of Pd NPs) of Pd/AIO(OH) towards the Buchwald–Hartwig coupling of amines with aryl halides under ligand-free aerobic condition.

XPS is a very handy tool to estimate the elements/components present in a sample [32–34]. The wide angle XPS spectra shown in Fig. 5a manifest that only Al, O and Pd are present in Pd/AIO(OH) catalyst. In other words, Pd/AIO(OH) catalyst is pure and free from other impurities. This obviously acknowledged the merit of the preparation procedure followed for the synthesis of Pd/AIO(OH) catalyst. A broad peak was observed in the binding energy range of 532–540 eV, which can be further deconvoluted into two peaks centred at 535 and 537.5 eV corresponding to O1s and Pd3p, respectively (Fig. 5b) [35, 36]. Similarly, in the high-resolution Al2p spectrum, the Al2p peak was located at 78 eV that exactly matches with the literature report (Fig. 5c) [37]. Two more peaks were identified

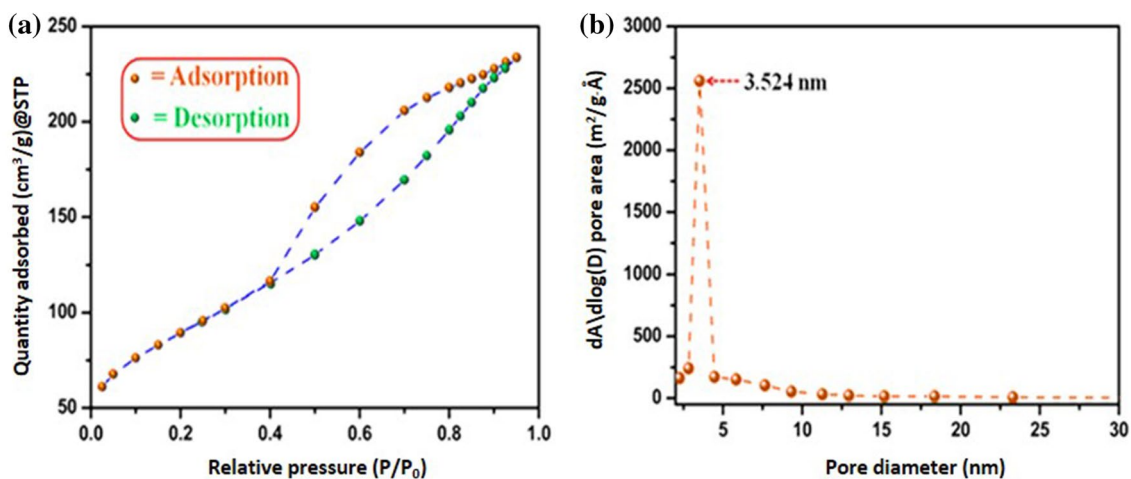


Fig. 4 **a** N_2 adsorption and desorption graph and **b** pore diameter distribution graph for Pd/AIO(OH)

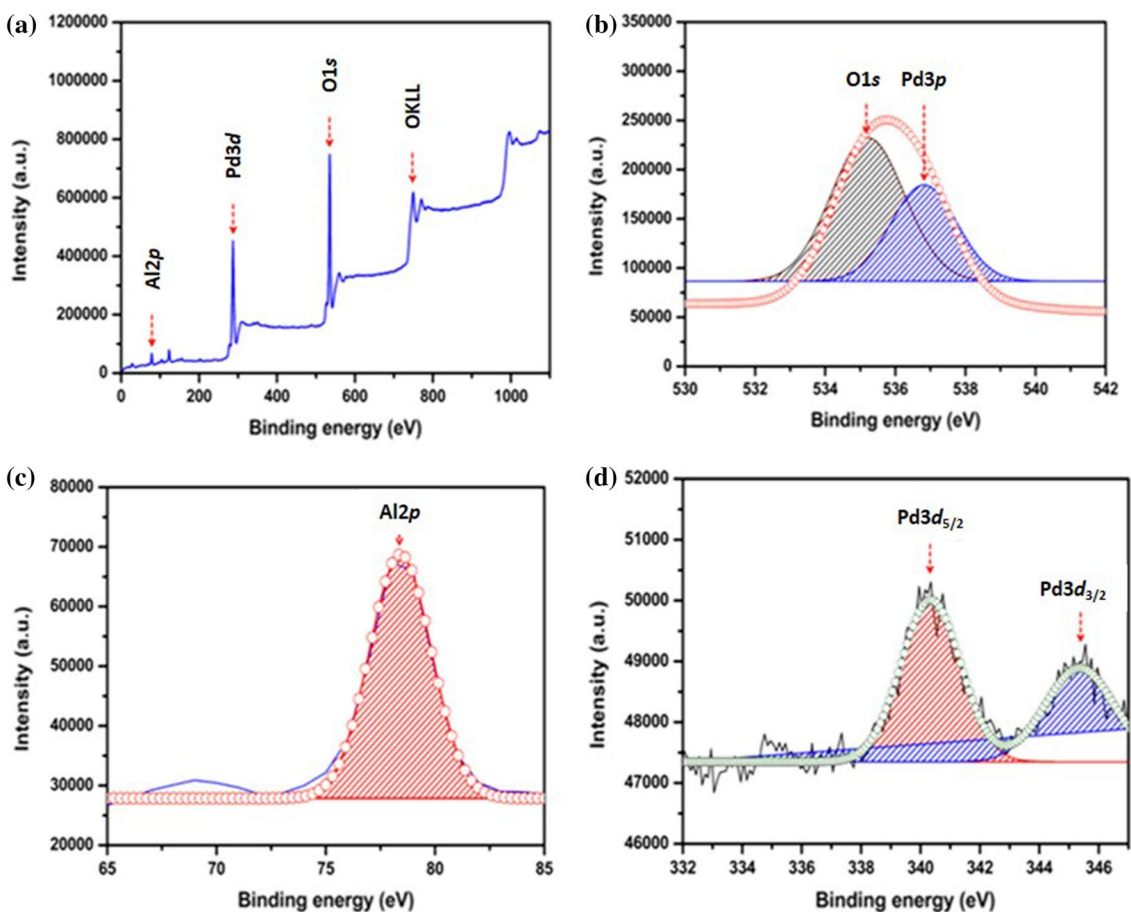


Fig. 5 **a** Wide angle, **b** high resolution O1s and Pd3p, **c** high resolution Al2p and **d** high resolution Pd3d XPS spectra of Pd/AIO(OH)

at 341.5 and 345.8 eV, which were evolved from Pd3d_{5/2} and Pd3d_{3/2} (Fig. 5d). Alike in previous reports, narrow peaks correspond to Pd3d_{5/2} and Pd3d_{3/2} were observed in

the high-resolution Pd3d spectrum, which confirmed the absence of Pd with higher chemical oxidation states [38]. Prominently, the XPS spectra supported the presence of zero

valent Pd NPs in Pd/AIO(OH) catalyst, which is in good agreement with the powder XRD results.

3.2 Optimization of Reaction Conditions

To get effective results, the reaction conditions were optimized. For this purpose, 4-chlorobenzonitrile (1 mmol) and aniline (1.2 mmol) were chosen as model substrates (Scheme 2). The completion of the reaction is monitored by gas chromatograph (GC). The process conditions such as solvent, base, catalyst amount and temperature were optimized to get a good yield and better catalytic system. Base plays a vital role in the C–N cross coupling reactions [39, 40]. Sunesson et al., studied the role of bases in Buchwald–Hartwig amination using density functional theory (DFT) [41]. Therefore, to find out the suitable base for the N-arylation of aniline, the reaction was carried out with different bases like potassium tertiary butoxide, potassium carbonate, potassium phosphate or potassium hydroxide (Fig. 6). The reaction with potassium phosphate showed a better yield; therefore, potassium phosphate was used as a base in the present system. Similarly, the influence of solvent in the reaction was studied as it played a major role in C–N cross coupling reactions [42]. The reaction was performed in different solvents like toluene, dimethyl formamide (DMF), dimethyl acetamide (DMAc) or dimethyl sulfoxide (DMSO) (Fig. 7). The results showed that DMSO was an appropriate solvent for this reaction. Alike, the reaction was conducted in the presence of varying amount of the catalyst (0, 0.15, 0.31 or 0.45 mol%) (Fig. 8). No progress in the reaction was observed in the absence of

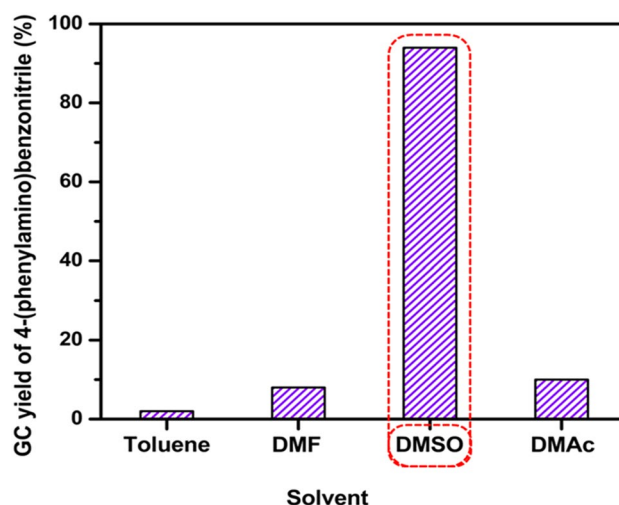


Fig. 7 Solvent optimization [Reaction conditions: 4-chlorobenzonitrile (1 mmol), aniline (1.2 mmol), Pd/AIO(OH) (0.31 mol%), K_3PO_4 (1.5 mmol), solvent (3 mL), 120 °C, 24 h]

Pd/AIO(OH) (0 mol%), which indicated the necessity of the catalyst in this reaction. However, the utmost product yield was achieved when the catalyst amount was 10 mg (0.31 mol%). Hence, it was taken as the optimized catalyst amount that was used for rest of the experiments. Besides, the reaction temperature optimization was done by carrying out the model reaction in the presence of Pd/AIO(OH) at different temperatures (Fig. 9). Generally, the Buchwald–Hartwig amination was performed at the temperature range of 100–150 °C [43, 44]. In our case, the highest yield was achieved at 120 °C; hence it was noted as the optimum reaction temperature.

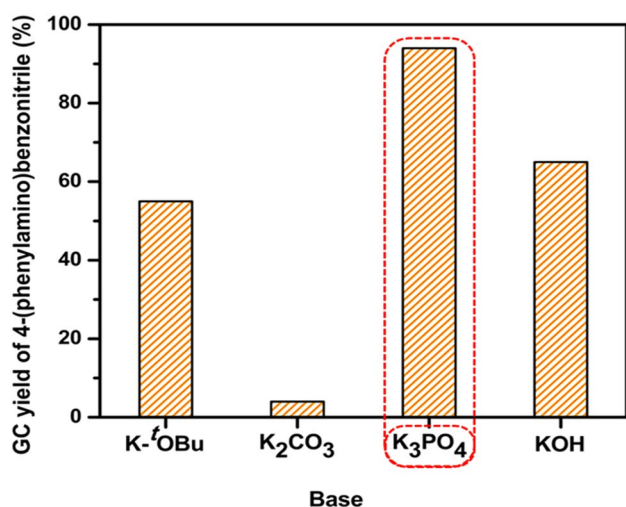


Fig. 6 Base optimization [Reaction conditions: 4-chlorobenzonitrile (1 mmol), aniline (1.2 mmol), Pd/AIO(OH) (0.31 mol%), base (1.5 mmol), DMSO (3 mL), 120 °C, 24 h]

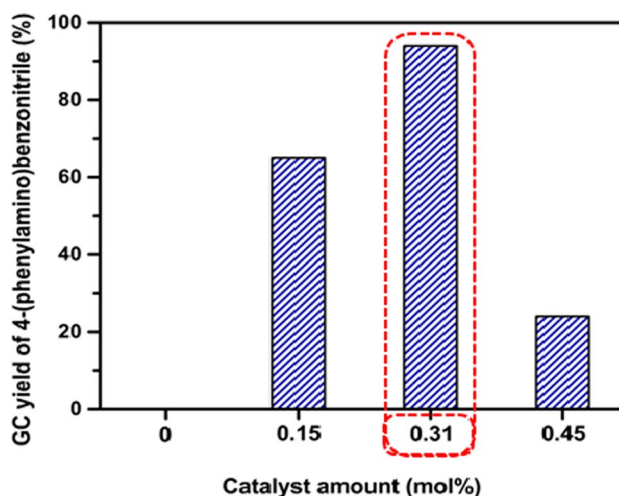


Fig. 8 Catalyst amount optimization [Reaction conditions: 4-chlorobenzonitrile (1 mmol), aniline (1.2 mmol), Pd/AIO(OH), K_3PO_4 (1.5 mmol), DMSO (3 mL), 120 °C, 24 h]

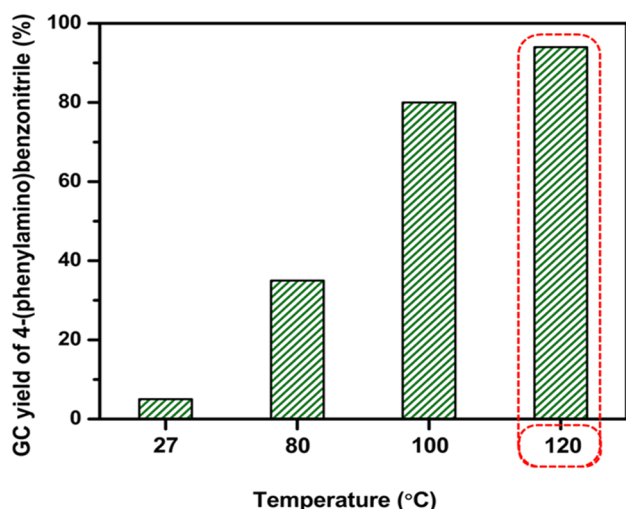


Fig. 9 Reaction temperature optimization [Reaction conditions: 4-chlorobenzonitrile (1 mmol), aniline (1.2 mmol), Pd/AIO(OH) (0.31 mol%), K_3PO_4 (1.5 mmol), DMSO (3 mL), 24 h]

3.3 Extension of Scope

The present protocol was extended to different aryl halides under optimized reaction conditions and the results are summarized in Table 1. Aniline reacted with 4-chlorobenzonitrile under ambient reaction conditions to yield 94% of the coupling product with very high turnover number (TON) of 303 (Table 1; entry 1). However, Hamann et al., demonstrated the utility of 2 mol% Pd(dba)₂ with 1,1'-bis(di-tert-butylphosphino)ferrocene as a ligand to yield only 79% of the same product at 110 °C after 16 h [45]. Likewise, CuI-catalyzed (10 mol%) homogeneous catalytic system gave only 81% of the same product after 24 h at 130 °C [46]. In general, the *para*-substituted aryl halides react much faster than the *ortho*-substituted ones. For illustration, the coupling of aniline with 4-chlorobenzonitrile gave 94% of the product (Table 1; entry 1), but the coupling of 2-chlorobenzonitrile yielded only 55% of 2-phenylamino benzonitrile with the TON and TOF of 177 and 7.4 h⁻¹, respectively (Table 1; entry 3). This can be justified by the steric hindrance in the case of *ortho*-substituted halides. On the other hand, [RhCp*Cl₂]₂/AgSbF₆ catalyzed the reaction homogeneously to afford 2-phenylamino benzonitrile in only 31% after 24 h at 120 °C under N₂ atmosphere [47]. Nonetheless, a similar trend was not observed in some of the bromo aryl systems. Both 4-bromobenzaldehyde and 2-bromobenzaldehyde exhibited similar reactivity with aniline to form 96% of the respective products with TON of 310 and TOF of 12.9 h⁻¹ (Table 1; entries 5–6). Likewise, 4-chlorobenzotrifluoride yielded 54% of the coupling product with the TON of 174 when it underwent reaction with aniline (Table 1; entry 4). As expected, aryl bromides are more reactive than

aryl chlorides. For example, 2-bromobenzonitrile gave 67% of the coupling product with aniline but 2-chlorobenzonitrile gave only 55% of the product (Table 1; entries 2–3). This might be owing to the better leaving group ability of bromide relative to chloride. It is well known that fluoride is the poorest leaving group in halides family [48]. Hence, the yield of coupling product of aniline with 4-fluorobenzaldehyde was much lesser (60%) than that of the coupling product evolved from 4-chlorobenzaldehyde (83%) (Table 1; entries 7–8). It is noted that 4-bromobenzaldehyde produced higher yield (96%) of the product compared to 4-chlorobenzaldehyde and 4-fluorobenzaldehyde (Table 1; entries 6–8). Further, the coupling of aniline with 2-bromoacetophenone yielded 85% of 1-(4-(phenylamino)phenyl)ethanone with the TON and TOF of 274 and 11.4 h⁻¹, respectively (Table 1; entry 9). But only 63% of the same product was produced by the coupling of iodobenzene with LiNH₂ and 4-iodoacetophenone in the presence of CuI (10 mol%) catalyst and K₃PO₄ base at 130 °C after 24 h [46]. In the same way, 4-bromobenzoic acid gave 70% of the desired coupling product with the TON and TOF of 226 and 9.4 h⁻¹, respectively (Table 1; entry 10).

Scope of the present system was extended to unsubstituted aryl halides and aryl halides with electron donating group to explore the versatility of Pd/AIO(OH). The present catalyst showed excellent activity for the coupling of aniline with bromobenzene, which gave 83% diphenyl amine (Table 1; entry 11). On the other hand, the same product (diphenyl amine) was obtained in only 78% yield after 36 h in presence of 5 mol% Pd(OAc)₂ catalyst using 1,10-phenanthroline (10 mol%) as a ligand under O₂ saturated toluene (0.5 mL) at 135 °C by aerobic amination of cyclohexanones with anilines [49]. Likewise, diphenyl amine was yielded by the coupling of phenyl tosylate and aniline in presence of 2 mol% Pd(OAc)₂, 5 mol% PhB(OH)₂, and a hindered and electron-rich MOP-type ligand (3 mol%) [50]. Largely, diphenyl amine is commercially manufactured by the thermal deamination of aniline using metal oxide catalyst. Hartwig and co-workers have utilized 5 mol% of (DPPF) PdCl₂ as a homogeneous catalyst for the coupling of 4-iodotoluene and aniline to produce the C–N coupling product in THF at 100 °C [51]. Nevertheless, only 0.31 mol% of Pd/AIO(OH) was used for the coupling of 4-bromotoluene and aniline to give 80% of the same product (Table 1; entry 12). The above results clearly revealed the wider employability of the catalyst.

3.4 Heterogeneity

Hot-filtration test was followed to analyze the heterogeneous nature of the catalyst and to prove the absence of leaching of Pd from boehmite [52, 53]. Pd/AIO(OH) was separated from the mixture of 4-chlorobenzonitrile, aniline and K₃PO₄ at 120 °C after attaining the product yield of

Table 1 Scope extension of Buchwald–Hartwig coupling reaction

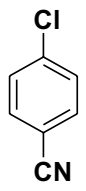
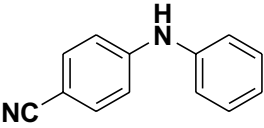
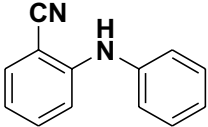
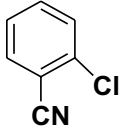
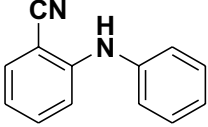
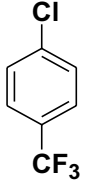
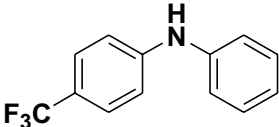
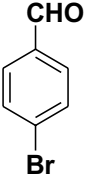
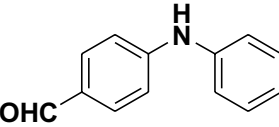
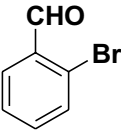
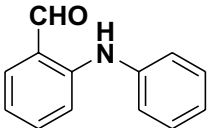
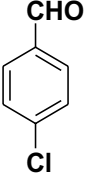
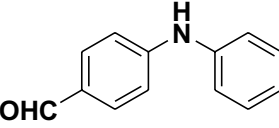
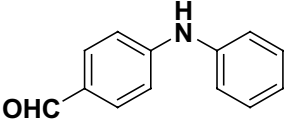
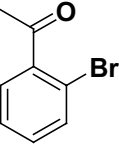
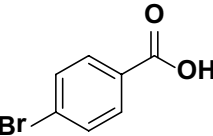
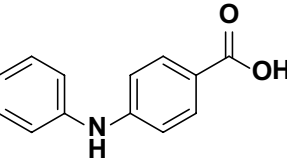
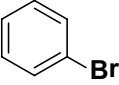
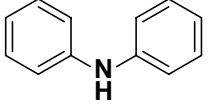
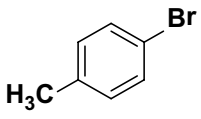
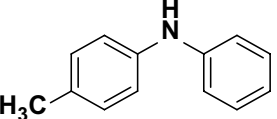
Entry	Aryl halide	Product	Yield ^a (%)	TON ^b /TOF (h ⁻¹) ^c
1			94	303/12.6
2			67	216/9.0
3			55	177/7.4
4			54	174/7.2
5			96	310/12.9
6			96	310/12.9
7			83	268/11.2

Table 1 (continued)

Entry	Aryl halide	Product	Yield ^a (%)	TON ^b /TOF (h ⁻¹) ^c
8			60	194 / 8.1
9			85	274 / 11.4
10			70	226 / 9.4
11			83	268 / 11.2
12			80	258 / 10.7

Reaction conditions: Aryl halide (1 mmol), aniline (1.2 mmol), Pd/AIO(OH) (0.31 mol%), K₃PO₄ (1.5 mmol), DMSO (3 mL), 120 °C, 24 h

^aDetermined by GC analysis

^bTurnover number (TON) = product (mol)/catalyst (mol)

^cTurnover frequency (TOF) (h⁻¹) = TON/Time in h

32% (after 12 h of reaction time), by centrifugation and allowed the reaction to proceed further without the catalyst. Then, the reaction was monitored in different time intervals (15, 18, 21 and 24 h). GC analysis showed that there was no increase in the yield of the product (Fig. 10) after the removal of the catalyst. The filtrate was analyzed by ICP-OES and a trace amount of Pd content of about 7 ppm was identified. Hence it is confirmed that the catalyst is of heterogeneous nature and stable during the reaction.

3.5 Reusability

Reusability is one of the major advantages of heterogeneous catalytic systems [54, 55]. After the completion of the reaction, the catalyst was recovered from the reaction mixture by centrifugation and washed with diethyl ether. Then, the recovered catalyst was used for the next cycles. The reaction was carried out for four times under identical conditions with recycled Pd/AIO(OH). The yield of product was 94% at the 1st run. No significant decrease was observed in the 2nd, 3rd and 4th runs as the yield of

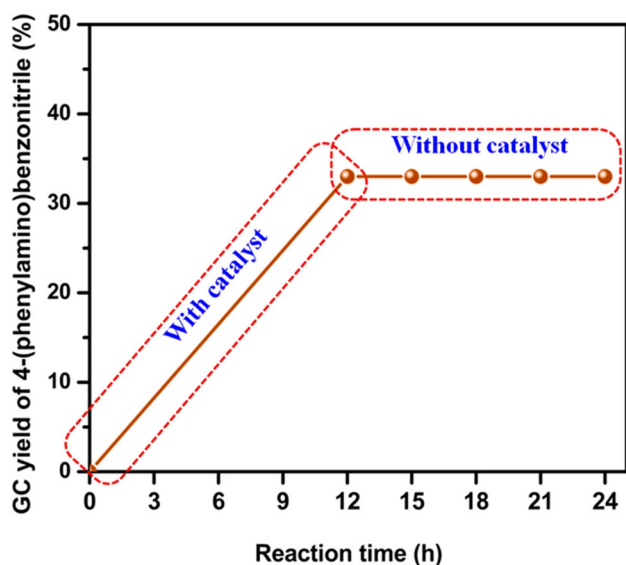


Fig. 10 Heterogeneity test [Reaction conditions: 4-chlorobenzonitrile (1 mmol), aniline (1.2 mmol), Pd/AIO(OH) (0.31 mol%), K_3PO_4 (1.5 mmol), DMSO (3 mL), 120 °C, 24 h]

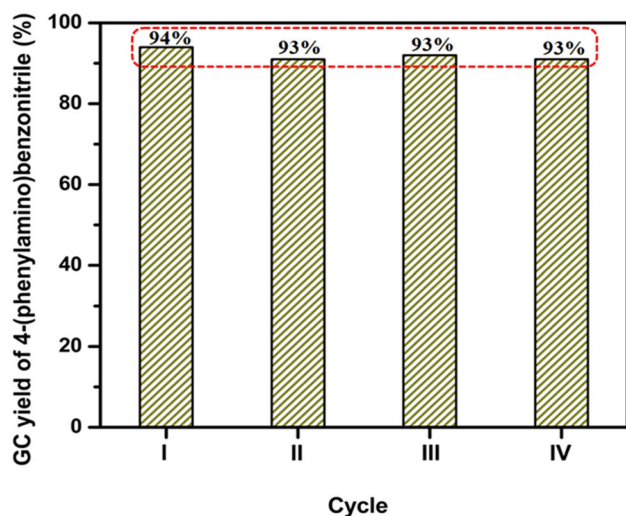


Fig. 11 Reusability test [Reaction conditions: 4-chlorobenzonitrile (1 mmol), aniline (1.2 mmol), Pd/AIO(OH) (0.31 mol%), K_3PO_4 (1.5 mmol), DMSO (3 mL), 120 °C, 24 h]

product was constantly maintained at 93% (Fig. 11). Furthermore, the recycled catalyst was examined by powder XRD. As can be seen from Fig. 12, the XRD pattern of the used catalyst is like that of fresh Pd/AIO(OH) (Fig. 1). Only difference observed between the two XRD patterns is the intensity. The used Pd/AIO(OH) showed less intense XRD peaks as compared to that of the fresh catalyst. These results indicated the excellent stability and reusability of Pd/AIO(OH).

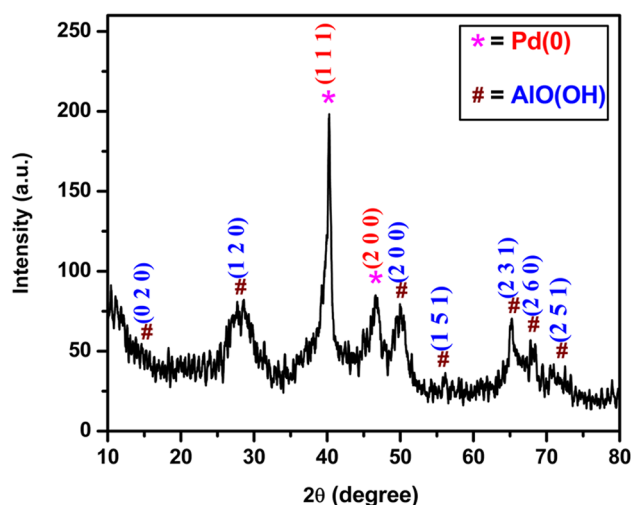


Fig. 12 Powder XRD pattern of the used Pd/AIO(OH)

4 Conclusions

A simple synthetic method for recyclable AIO(OH)-supported Pd NPs catalyst was developed from readily available reagents and its high activity towards the N-arylation of aniline was demonstrated. The smaller size (10 nm) of metallic Pd NPs, and wafer structure, nano porous nature and high surface area of AIO(OH) made this catalytic protocol efficient. Essentially, the Buchwald–Hartwig cross coupling was performed using less amount of Pd (0.31 mol%) with high TON and TOF. Coupling of aniline with different kind of aryl halides was successfully performed under simple operating conditions. This catalytic system is expected to be applicable for preparing different substituted aromatic amines with very good yield. The catalyst is truly heterogeneous, reusable and stable. Notably, this amination protocol can be performed under ligand-free and aerobic conditions.

Acknowledgements R.K. acknowledges DAE-BRNS for the financial support.

References

1. Kates SA, Albericio F (2000) Solid-phase synthesis: a practical guide. Marcel Dekker, New York, pp 419–473
2. Brown BR (1994) The organic chemistry of aliphatic nitrogen compounds. Oxford University Press, New York, pp 217–221
3. Brandani S, Brandani V, Vegliò F (1998) Ind Eng Chem Res 37:292–295
4. Shen C, Wang L, Wen M, Shen H, Jin J, Zhang P (2016) Ind Eng Chem Res 55:3177–3181
5. Navarro O, Kaur H, Mahjoor P, Nolan SP (2004) J Org Chem 69:3173–3180
6. Dai Q, Gao W, Liu D, Kapes LM, Zhang X (2006) J Org Chem 71:3928–3934
7. Parrish CA, Buchwald SL (2001) J Org Chem 66:3820–3827

8. Vagheia RG, Hemmatia S, Hamelian M, Veisi H (2015) *Appl Organometal Chem* 29:195–199
9. Veisi H, Heravi MRPH, Hamelian M (2015) *Appl Organometal Chem* 29:334–337
10. Veisi H, Morakabati N (2015) *New J Chem* 39:2901–2907
11. Ghotbinejad M, Khosropour AR, Moghadam M, Tangestaninejad S, Mirkhani V (2016) *Nano Chem Res* 1:40–48
12. Al-Amin M, Honma T, Hoshiya N, Shuto S, Arisawa M (2012) *Adv Synth Catal* 354:1061–1068
13. Kim S, Bae SW, Lee JS, Park J (2009) *Tetrahedron* 65:1461–1466
14. Park IS, Kwon MS, Kim N, Lee JS, Kang KY, Park J (2005) *Chem Commun* 3:5667–5669
15. Babu SG, Priyadarsini PA, Karvembu R (2011) *Appl Catal A Gen* 392:218–224
16. Babu SG, Thomas B, Nijamudheen A, Datta A, Karvembu R (2012) *Catal Sci Technol* 2:1872–1878
17. Chang F, Kim H, Lee B, Park S, Park J (2010) *Tetrahedron Lett* 51:4250–4252
18. Chang F, Kim H, Lee B, Park HG, Park J (2011) *Bull Korean Chem Soc* 32:1074–1076
19. Han K, Park J, Kim MJ (2008) *J Org Chem* 73:4302–4304
20. Jeon M, Han J, Park J (2012) *ChemCatChem* 4:521–524
21. Göksu H (2015) *New J Chem* 39:8498–8504
22. Kwon MS, Kim S, Park S, Bosco W, Chidrala RK, Park J (2009) *J Org Chem* 74:2877–2879
23. Kwon MS, Kim N, Seo SH, Park IS, Cheedrala RK, Park J (2005) *Angew Chem Int Ed* 44:6913–6915
24. Song J, Li Z, Xu X, He M, Li Z, Wang Q, Yan L (2013) *Ind Eng Chem Res* 2:6–11
25. Gong X, Nie Z, Qian M, Liu J, Pederson LA, Hobbs DT, McDuffie NG (2003) *Ind Eng Chem Res* 42:2163–2170
26. Kumar PR (2012) *J Biomater Nanobiotechnol* 3:14–19
27. Venkatesan P, Santhanalakshmi J (2011) *Nanosci Nanotechnol* 1:43–47
28. Hou HW, Zhu Y, Hu QY (2013) *Mater Trans* 54:1686–1690
29. Wang C, Han L, Zhang Q, Li Y, Zhao G, Liu Y, Lu Y (2015) *Green Chem* 17:3762–3765
30. Zhao B, Wang Q, Zhang S, Deng C (2015) *J Mater Chem A* 3:12089–12096
31. Lu CL, Lv JG, Xu L, Guo XF, Hou WH, Hu Y, Huang H (2009) *Nanotechnology* 20:215604
32. Babu SG, Vinoth R, Praveen Kumar D, Shankar MV, Chou H-L, Vinodgopal K, Neppolian B (2015) *Nanoscale* 7:7849–7857
33. Babu SG, Vinoth R, Neppolian B, Dionysiou DD, Ashokkumar M (2015) *J Hazard Mater* 291:83–92
34. Gopiraman M, Bang H, Babu SG, Wei K, Karvembu R, Kim IS (2014) *Catal Sci Technol* 4:2099
35. Ketteler G, Ogletree DF, Bluhm H, Liu H, Hebenstreit ELD, Salmeron M (2005) *J Am Chem Soc* 127:18269–18273
36. Babu SG, Neelakandeswari N, Dharmaraj N, Jackson SD, Karvembu R (2013) *RSC Adv* 3:7774–7781
37. Neelakandeswari N, Sangami G, Emayavaramban P, Babu SG, Karvembu R, Dharmaraj N (2012) *J Mol Catal A Chem* 356:90–99
38. Li X, Ouyang J, Zhou Y, Yang H (2015) *Sci Rep* 5:13763
39. Babu SG, Karvembu R (2011) *Ind Eng Chem Res* 50:9594–9600
40. Gopiraman M, Babu SG, Khatri Z, Kai W, Kim YAYA, Endo M, Karvembu R, Kim IS (2013) *Carbon* 62:135–148
41. Sunesson Y, Lime E, Lill SON, Meadows RE, Norrby P-O (2014) *J Org Chem* 79:11961–11969
42. Jerome P, Kausalya G, Daniel Thangadurai T, Karvembu R (2016) *Catal Commun* 75:50–54
43. Fors BP, Buchwald SL (2011) *J Am Chem Soc* 132:15914–15917
44. Shen Q, Hartwig JF (2008) *Org Lett* 10:4109–4112
45. Hamann BC, Hartwig JF (1998) *J Am Chem Soc* 120:7369–7370
46. Tlili A, Monnier F, Taillefer M (2012) *Chem Commun* 48:6408
47. Dong J, Wu Z, Liu Z, Liu P, Sun P (2015) *J Org Chem* 80:12588–12593
48. Sivakami R, Babu SG, Dhanuskodi S, Karvembu R (2015) *RSC Adv* 5:8571–8578
49. Girard SA, Hu X, Knauber T, Zhou F, Simon MO, Deng GJ, Li CJ (2012) *Org Lett* 14:5606–5609
50. Xie X, Ni G, Ma F, Ding L, Xu S, Zhang Z (2011) *Synlett* 2011:955–958
51. Driver MS, Hartwig JF (1996) *J Am Chem Soc* 118:7217–7218
52. Gopiraman M, Babu SG, Khatri Z, Kai W, Kim YA, Endo M, Karvembu R, Kim IS (2013) *J Phys Chem C* 117:23582–23596
53. Babu SG, Krishnamoorthi S, Thiruneelakandan R, Karvembu R (2014) *Catal Lett* 144:1245–1252
54. Babu SG, Karvembu R (2013) *Tetrahedron Lett* 54:1677–1680
55. Babu SG, Vinoth R, Surya Narayana P, Bahnemann D, Neppolian B (2015) *APL Mater* 3:104415